Colloids and Surfaces A: Physicochem. Eng. Aspects 412 (2012) 82–89

Contents lists available at SciVerse ScienceDirect

Colloids and Surfaces A: Physicochemical and Engineering Aspects

journal homepage: www.elsevier.com/locate/colsurfa

Enhanced diamond nucleation on copper substrates by employing an electrostatic self-assembly seeding process with modified nanodiamond particles

Xuezhang Liu[a], Tao Yu[a], Qiuping Wei[a,b,*], Zhiming Yu[a,b], Xiangyang Xu[c]

[a] *School of Materials Science and Engineering, Central South University, Changsha, 410083, PR China*
[b] *State Key Laboratory of Powder Metallurgy, Central South University, Changsha, 410083, PR China*
[c] *R & D, Changsha Research Institute of Mining and Metallurgy, Changsha, 410083, PR China*

HIGHLIGHTS

- Surface modification and fractionalization prepared a nanodiamond colloid.
- Two-dimensional self-assemblies of nanodiamond seeding without any contaminations.
- The seeding process was revealed from the nonlinear Poisson–Boltzmann theory.
- The interaction energies between ND particle and Cu substrate were calculated.
- High quality of 800 nm thick continuous diamond film was deposited in 60 min.

GRAPHICAL ABSTRACT

By adopting the nonlinear Poisson–Boltzmann theory, the electrostatic energy in the seeding process was calculated, where $a_2 = 25.3$ nm, and the measured zeta potentials of $\xi_1 = -41.5$ mV, $\xi_2 = 70.7$ mV for nanodiamond particles and copper substrate, respectively, at pH 6.7, are used in the analysis. As the curve shown, when the distance between nanodiamond particles and copper substrate decreases, the value of the electrostatic energy exponentially increases.

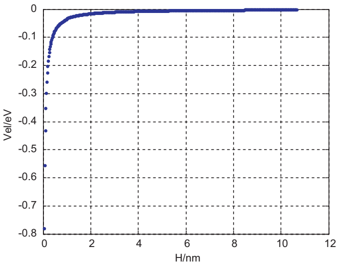

ARTICLE INFO

Article history:
Received 28 March 2012
Received in revised form 25 May 2012
Accepted 11 July 2012
Available online 26 July 2012

Keywords:
Nanodiamond seeding
Surface modification
CVD diamond film
Electrostatic self-assembly
Interaction energy
Copper substrate

ABSTRACT

Nanodiamond seeding is a well-established approach to enhancing the nucleation density in chemical vapor deposition (CVD) diamond growth. However, the effects of nanodiamond seeding are highly dependent upon the dispersion properties of nanodiamond particles, the solvent and the interaction between nanoparticles and substrate surfaces. Surface modification and fractionalization were employed to improve the dispersion of nanodiamond particles and separate those particles into a more narrow range of particle size. Mono-dispersed nanodiamonds with a ζ-potential and average particle size of −41.5 mV and ~25.3 nm, respectively, were then obtained. They can be charged on copper substrate without any contaminations. Two-dimensional self-assemblies of nanodiamond seeding were actualized. The density and homogeneity of nanodiamond particles which act as pre-existing sp^3 seeds shorten the incubation time of diamond nucleation to less than 30 min. High quality of 750 nm thick continuous diamond film was deposited on copper substrate in 60 min. Furthermore, we calculated electrostatic interaction energy between nanodiamond particle and copper substrate by using the nonlinear Poisson–Boltzmann theory, and discussed interaction energy of nanodiamond-Cu substrate and nanodiamond–nanodiamond in the seeding process.

1. Introduction

CVD diamond deposition on non-diamond substrates requires surface treatment in order to achieve a high nucleation density [1]. One of the most widely used approaches is seeding the substrate with diamond particles dispersed in an appropriate solvent

---

[*] Corresponding author at: School of Materials Science and Engineering, Central South University, Changsha, 410083, PR China. Tel.: +86 731 88830335; fax: +86 731 88876692.
E-mail addresses: qiupwei@csu.edu.cn (Q. Wei), zhiming@csu.edu.cn (Z. Yu).

0927-7757/$ – see front matter © 2012 Elsevier B.V. All rights reserved.
http://dx.doi.org/10.1016/j.colsurfa.2012.07.020

accompanied by ultrasonic agitation [2–4]. Nanodiamond (ND) particles have been shown to provide the highest nucleation density as compared to ultrasonic treatment with particles of larger size [4]. Furthermore, ND seeding can cover complex surfaces, including porous structures [5] and 3D nano/micro-electromechanical systems (N/MEMS), avoid inducing mechanical damage and provide high precision during creation of seeded patterns on the substrate [6]. Girard et al. [7] reported that nanocrystalline diamond films of 70 nm thick had been obtained by electrostatic grafting of ND on cationic polymer-coated silicon substrate.

On one side, ND particles, produced from carbon-containing explosives, have a nano-scaled diameter. They can easily aggregate during synthesis and subsequent treatments, especially when added into a variety of solvent. Consequently, further de-agglomeration and dispersion are necessary [8,9]. On the other size, ND seeding is a complicated system since it involves ND particles, dispersion solvent and the substrate. Though mono-dispersed ND is adopted, larger aggregation still forms during drying process, which may originate from the mismatch of surface properties between ND particles and the substrate or low dispersion stability of ND colloid. The uneven seeding will decrease seeding density and damage the homogeneity of diamond film.

Mendes de Barros et al. [10] have compared the effects of several dispersion liquids on diamond seeding from five key liquid properties such as: dipole moment, density, vapor pressure, surface tension and viscosity. The results identified that n-hexane and n-pentane are the most suitable liquids. Shenderova et al. [11] demonstrated that combination of dimethyl sulfoxide (DMSO) and alcohol as seeding solvent allowed the removal of the solvent without damaging the uniformity of ND seeds after they distributed over a substrate.

Therefore, in order to achieve homogenous seeding in CVD diamond growth, ND surface chemistry, colloidal stability, the interaction energy between ND particles and the substrate are needed to be overall investigated.

Due to its extreme mechanical, thermal and electrical properties, CVD diamond deposition on copper substrate has attracted many interests. Since copper is immiscible with carbon, graphite layers are needed to be produced as intermediate, which requires a very long induction time (>10 h) [12,13]. This special nucleation kinetics resulted into low nucleation density [14,15].

Because of these factors, ND particles were modified and fractionated to seed the copper substrates. Those ND particles with negative ζ-potential can be charged on copper substrate. This self-assembly method will reach the ideal seeding case: a compact layer of ND particles homogeneously dispersed on the copper substrate. Diamond films deposited later presented high quality with incubation time shorter than less than 30 min.

2. Experimental details

2.1. Surface modification and fractionalization of nanodiamond

ND particles were loaded in the crucible, then put in the stove and heated in air atmosphere within the temperature range of 725–750 K for 30 min. Before taken out for further investigations, the samples were cooled along with the stove under the surrounding room temperature. Following the heat treatment, ND particles were dispersed in de-ionized water using a direct-immersion horn-type ultrasound sonicator (output power of 100–400 W) [16,17]. Then, the ND suspension was further fractionated by a multipurpose refrigerated centrifuge (Thermo Electron Corporation). At the end of fractionation, the supernatant was diluted with an aqueous 0.001 M KCl solution to 0.05 wt% concentration, and subjected to sonication bath to obtain a stable colloid (KCl is an inert electrolyte).

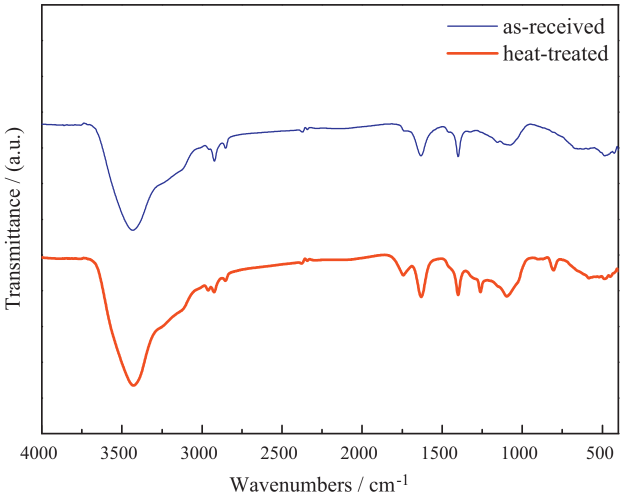

Fig. 1. FTIR spectra of as-received and heat-treated sample.

Fourier transform infrared (FTIR) spectroscopy was introduced to analyze the functional groups on ND surfaces, using the standard technique of KBr-pellet with Nexus 470 (Thermo Nicolet, USA). ND particles were dehydrated before the analysis. Malvern Zetasizer Nano ZS (Malvern Instruments Ltd., UK) was adopted for measurement of the particle size.

2.2. Electrostatic self-assembly seeding

For electrostatic self-assembly seeding, cleaned copper substrates were immersed in the aforementioned colloid for 10 min. The copper substrates taking positive ζ-potentials in 0.001 M KCl solution and ND with negative ζ-potentials facilitate the rapid formation of a nanoseeding layer. The copper substrates were then rinsed in de-ionized water, and blow-dried. After those processes, only those particles which have strong interaction with the substrate were remained.

Electrokinetic measurements of copper substrate and ND particle were carried out in 0.001 M KCl solution with an EKA electrokinetic analyzer from Anton Paar (Graz, Austria) [18]. Hydrochloric acid and sodium hydroxide were used as regulators to modify pH value of the aqueous solution. The zeta-potential values were calculated from the measured streaming potentials by using the Smoluchowski equation.

2.3. Diamond films deposition

Diamond films deposition were carried out in a hot filament chemical vapor deposition (HF-CVD) system which has been described elsewhere [19]. The normal growth conditions were: methane concentration, 2%; hydrogen, 98%; deposition pressure, 3 kPa; substrate temperature, 1023 ± 50 K.

Samples were characterized by field-emission scanning electron microscopy (FE-SEM FEI, Sirion200) and Raman spectroscopy (LabRAM HR800, Ar^+ ion laser operating at 488 nm with an output power of 100 mW), respectively.

3. Results and discussion

3.1. Surface functional groups

The transformation of surface functional groups on ND is shown in Fig. 1. As a result of heat treatment, the FTIR spectrum of ND becomes smooth, confirming higher uniformity in the composition of sample surface. The absorption peak at 1742.60 cm^{-1}

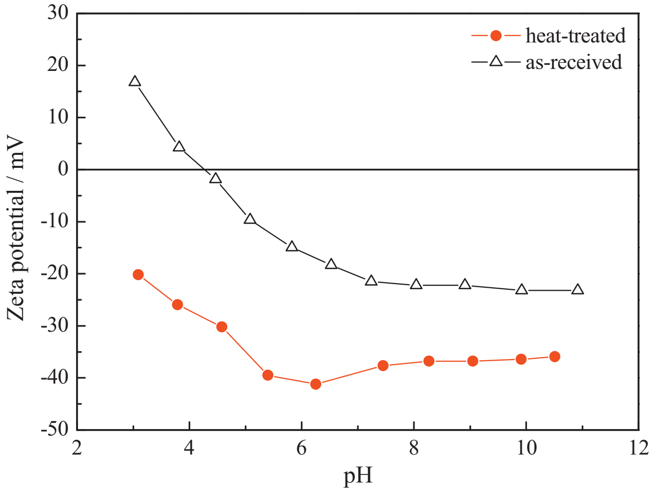

Fig. 2. Zeta potential vs pH of as-received and heat-treated sample.

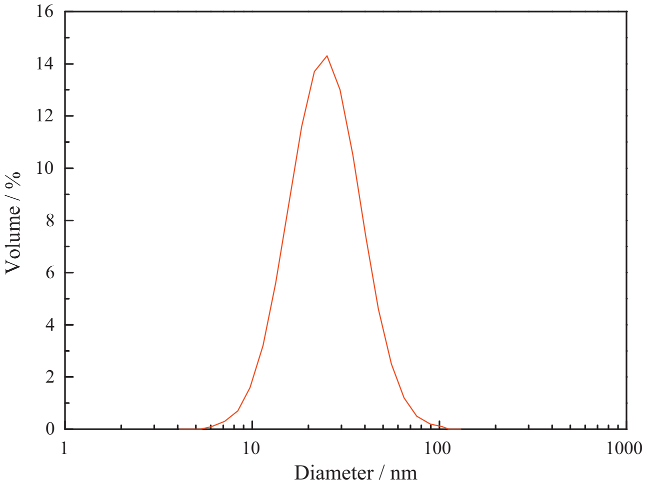

Fig. 3. Particles size distribution after heat treatment and fractionation process (in de-ionized water, pH: 6.54).

corresponds to the C=O stretching vibration of carbonyl groups. And the absorption peak at 1260.93 cm^{-1} corresponds to the vibration of ether groups (—C—O—C—). As expected, heat treatment increases the intensities of these peaks.

The strengthening of C=O stretching vibration of carbonyl groups can mainly be attributed the rupture of hydrogen bands and the oxidation of alkane hydrocarbon groups [20]. The strengthening of ether groups vibration (—C—O—C—) may be caused by cyclic ketone (band in between 1700 and 1800 cm^{-1}) and lactone (lactone C=O features band positioned in between that for ketone and carboxylic anhydride) formation between adjacent ND particles during the heating [21].

The absorption peaks at 2924.65 and 2854.25 cm^{-1} correspond to the asymmetric and symmetric stretching C—H vibration respectively. And the strong and broad absorption peak at 3428.10 cm^{-1} corresponds to the stretching O—H vibration and amino-groups stretching vibration, while that at 1631.03 cm^{-1} corresponds to the bending O—H vibration and deformation N—H vibration. Heat treatment results in the decline of the intensity of these peaks.

3.2. Surface electrical property

Fig. 2 shows the change of zeta potential of ND particles in de-ionized water. According to the zeta potential measurement, as-received sample is positively charged in acidic medium and the isoelectric point (IEP) is located at 4.2. After heat treatment, the zeta-pH curve shifts downward, and no IEP is observed, ND particles are negatively charged in the whole observed pH range.

For ND powders, surface functional groups originated from the chemical treatment processing impart a charge to ND particles in aqueous solution. The value and sign of this charge depend on the concentration and dissociation constant of these groups, the solution pH and the background-electrolyte concentration. In our study, H^+ and OH^- are potential-determining, which can be attributed to the protonation of amino-groups and the deprotonation of carboxyl respectively [22]. The results of Fig. 2 verify the composition change of surface functional groups, i.e. the oxidation of some surface groups such as hydrocarbon groups increasing the relative amount and density of carboxyl on ND surface. When a large amount of carboxyl groups are formed on the ND surface by heat treatment, the deprotonation of carboxyl will be still dominant in acidic media, and then ND particles can be strongly negatively charged in the whole observed pH range.

3.3. Dispersion in aqueous medium

As-received sample is firstly dispersed in de-ionized water. Particle size measurement by dynamic light scattering (DLS) method shows that it is a typical poly-dispersed, which indicates poor resistance to agglomeration and sedimentation of ND in suspensions (not shown). The average particle size varies between 200 and 400 nm with a small amount (~2 wt %) of micron-sized agglomerated particles. After centrifuged at 2000 × g for 5 min, up to 80% of ND is spread along the centrifuge tube side wall. Apparently, it is not suitable to fractionate ND into smaller-sized fractions by centrifugation.

In comparison, heat-treated sample forms very stable suspensions in de-ionized water after sonication. After multi-step centrifugation, small nanoparticles are isolated from ND particles. Fig. 3 illustrates the corresponding distribution of particle size. It reveals that the colloidal particles have an average particle size of 25.3 nm. No micron and submicron aggregates are observed. Obviously, the ND colloid is highly dispersed and appropriate for seeding. Heat treatment and fractionation process have successfully decreased the large particles to their core size. A milling process can also control the surface termination of ND particles and obtain a stable colloid. But ND particles were unavoidable contaminated by milling beads and surfactants [16], though the negative effects of those impurities on sequent diamond nucleation and growth were never investigated [7,23].

According to the well-known Derjaguin–Landau–Verwey–Overbeek (DLVO) theory, colloidal stability is governed by the total interparticle interaction energy ($V(H)$) at a given interparticle separation distance, H.

$$V(H) = V_R(H) + V_A(H) \tag{1}$$

where $V_A(H)$ is an attractive potential arising from long-range van der Waals forces, $V_R(H)$ is a repulsive potential due to electrostatic forces. Electrostatic forces give rise to repulsive interactions between like-charged colloidal particles suspended in a polar solvent. For moderate surface potentials $V_R(H)$ is given by

$$V_R(H) = 2\pi\varepsilon\varepsilon_r a\xi^2 \ln(1 + e^{-\kappa H}) \tag{2}$$

where κ is the Debye parameter, ξ is the zeta-potential. From the Eq. (2), it is known that the increased absolute value of ξ after heat treatment enhanced the electrostatic repulsion between particles, then after ultrasonic agitation, ND particles can stay stable in the suspension. Normally, ND particles with the absolute value

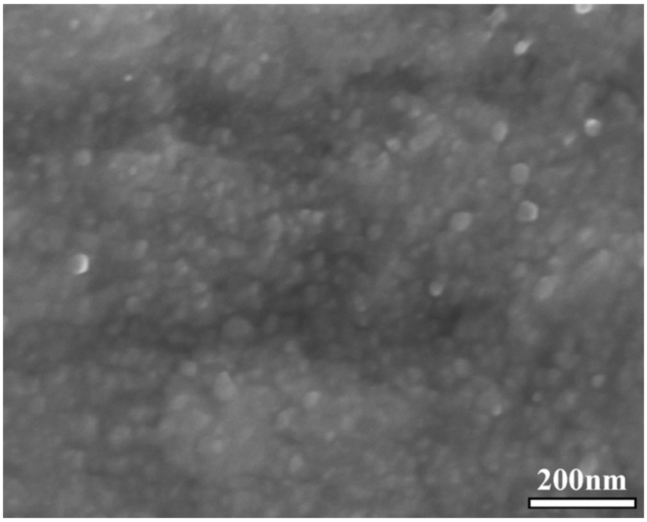

Fig. 4. SEM image of two-dimensional self-assemblies of nanodiamond seeding on Cu substrate.

of ξ more than 30 mV can balance the thermal energy of the particles which results in aggregation. From the analysis of ND surface electrical property, the dispersions of heat treated samples in de-ionized water can be stable within pH range of 4.23–10.57.

3.4. Electrostatic self-assembly seeding

Since copper is an excellent conduct metal. We can observe the individual ND particles charged on the seeding surface directly. As shown in Fig. 4, a mono-dispersed nanoparticle seeding is obtained though the substrate topography is wavy and out-of-flatness. The coverage of the copper substrate is highly uniform and in high density. No distinct aggregate is visible. The size of individual particles is in the range of 20–30 nm, which is comparable with DLS measurements. In this case, the nucleation density calculated by counting the total number of diamond seed crystallites and divided by the area is greater than 10^{11} cm^{-2} since multiple nucleation can take place at a single particle, which is two orders of magnitude higher than those results reported in literatures about diamond films deposited on copper substrate [14,15].

Shenderova et al. [11] found that seeding on silicon wafer by using the nanodiamond dispersed in pure DMSO produced many aggregates because of its high surface tension, high boiling point and slow evaporation at normal atmospheric pressures. But this phenomenon does not present in our experiment even the dispersion medium is de-ionized water, which presents higher surface tension, higher boiling point and slower evaporation than DMSO. The difference can be attributed to the corresponding interaction energy between ND particles and substrate surface.

The calculated electrostatic energy (V_R (H)) between nanodiamond particle and copper substrate in the present seeding system is shown in Fig. 5. ($V_R(H)$) is given by Eq. (12) (Appendix), where $a_2 = 25.3$ nm, and the measured zeta potentials of $\xi_1 = -41.5$ mV, $\xi_2 = 70.7$ mV for ND particles and copper substrate, respectively, at pH 6.7, are used in the analysis. Meanwhile, we use 0.001 M as the electrolyte concentration which is corresponding to $\kappa = 1.46 \times 10^8$ m^{-1}. The boundary conditions in our seeding system satisfy condition I(C) in [24]. As illustrated in Fig. 5, V_R (H) represents net attractive interactions. When the interaction distance decreases, V_R (H) increases exponentially.

To obtain the van der Waals energy (V_A (H)) between nanodiamond particle and copper substrate, we make use of the approach proposed by *Lifshitz*. For a sphere (1)-plate (3) system with intervening medium (2) separated by distance H, the interaction energy of van der Waals is given by [25]

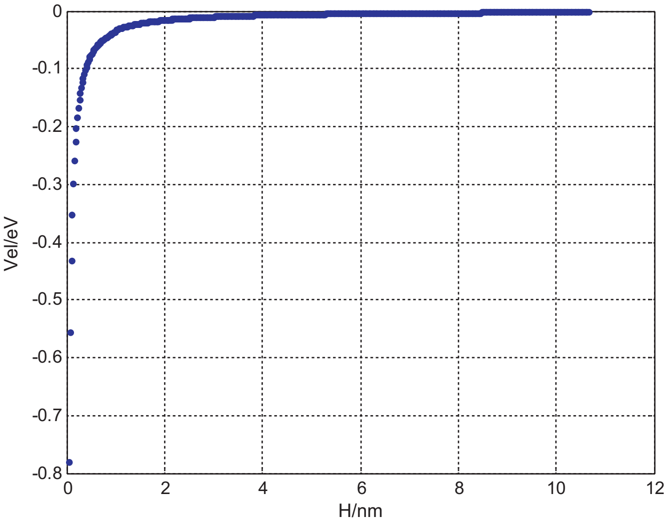

Fig. 5. The calculated electrostatic energy between ND particles and Cu substrate.

$$V_A(H) = -\frac{A_{123}R}{6H}, \tag{3}$$

$$A_{123} \approx \left(\sqrt{A_{11}} - \sqrt{A_{22}}\right)\left(\sqrt{A_{33}} - \sqrt{A_{22}}\right), \tag{4}$$

where R is the radius of a sphere and A_{123} is a unique *Hamaker* constant for the triple system. Unfortunately, substituting Hamaker constants of nanodiamond particle and copper substrate with 29.6×10^{-20} J [26] and 40×10^{-20} J [27], the calculated value is much larger than V_R (H). It implies that the nanoseeding efficiency is very high regardless of whether there is an electrostatic attractive interaction. This calculated result obviously contradicts with experimental works (Hamaker constant of Si is 25.6×10^{-20} J [27], and the corresponding A_{123} for Si/H_2O/ND system is close with the one for Cu/H_2O/ND system) [6,7,23,28,29]. For example, in [29], XPS spectra showed the surface covered by nanodiamond particles were estimated at 51%. Furthermore, the measured van der Waals interaction weaker than predicted is generally reported in literatures [30–33]. Giesbers et al. [34] studied the interactions between a film surface and a sphere by atomic force microscope. For all systems investigated (silica–silica, gold–gold, and silica–gold), measured interactions were found to be entirely due to overlap of electric double layers with no indication of attractive Van der Waals forces. The experimental data are in between the (fitted) theoretical curves for the boundary conditions of constant charge and constant potential, respectively. They attributed the deviation to surface roughness and solvent structural forces (repulsion between hydration layers).

The factors resulted into the deviation in our ND/Cu system are follows: (1) the sp^2 fullerene-like layer on particle surface makes the *Hamaker* constant of diamond nanoparticle different from bulky diamond [35]. π-electrons of graphitic partial surface affects optical absorption [16]. (2) The nanoscale size causes a deviation to *Hamaker* constant [36]. (3) Modified diamond nanoparticles present abundant polar interaction with dispersed medium, including hydrogen bonding, protonation of amino-groups and deprotonation of carboxyl. (4) The surface roughness of Cu substrate.

From the above discussion, we can find that the calculation of van der Waals interaction is complicated since it needs to be corrected by a larger number of measured data. Those results will be presented in another paper.

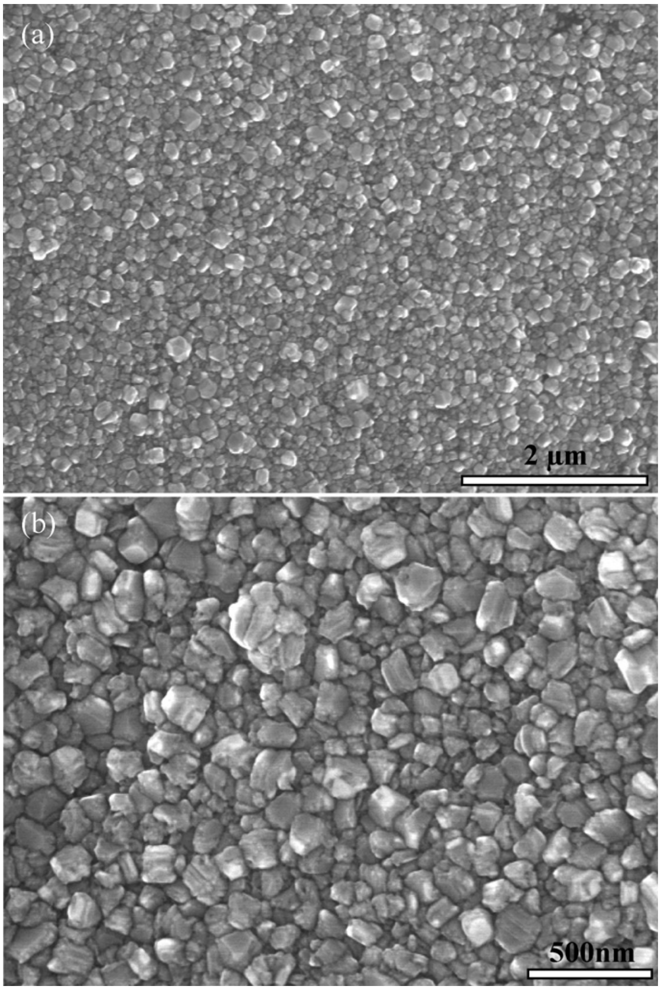

Fig. 6. (a) SEM image of the diamond film deposited for 30 min; (b) an enlargement SEM image of the diamond film deposited for 30 min.

All in all, a net attractive interaction promotes ND particles charged on Cu substrate. The efficient interaction between ND particles and Cu substrate is evidenced by the stability of the ND particles upon rinsing in de-ionized water (Fig. 4). At the same time, the repulse interaction among ND particles hinders their aggregation, and the attached particles also repulsed others to charge on Cu substrate. Therefore, two-dimensional self-assemblies of nanodiamond seeding particle are obtained. Those results coincide with the work in [28]. They have reported that the intrinsic negative charge of 500 nm diamond particles allows the formation of two-dimensional assemblies by electrostatic adsorption on poly(diallyldimethylammonium chloride) modified In-doped SnO_2 electrodes. The particle number density in the assembly was controlled by the adsorption time. However, the effect of absorption time is not obvious in our experiments. During electrostatic self-assembly seeding process, we do find that the particle number adsorbed on Cu substrate depends on the pH value of aqueous suspension. This phenomenon implies that assembly efficiency is related with the interaction energy between ND particles and Cu substrate. Malysheva et al. [37] investigated the adhesion between a charged particle in an electrolyte solution and a charged substrate. They found that the equilibrium separation between the particle and the substrate was affected by the surface charge of the substrate, while equilibrium separation was determined by calculating the sum of electrostatic and van der Waals free energies. What deserves special attention here is that we substituted zeta potential for reduced potential in the calculation of electrostatic energy. In order to obtain more accurate calculations, the ionization of intrinsic surface groups must be combined into the ionization of ion binding as described in the Gouy–Chapman–Stern–Grahame (CGSG) model [38]. Surface charge data such as the potential, the capacitances (per unit area) of the inner layer and outer layer are derived from precise titration experiments.

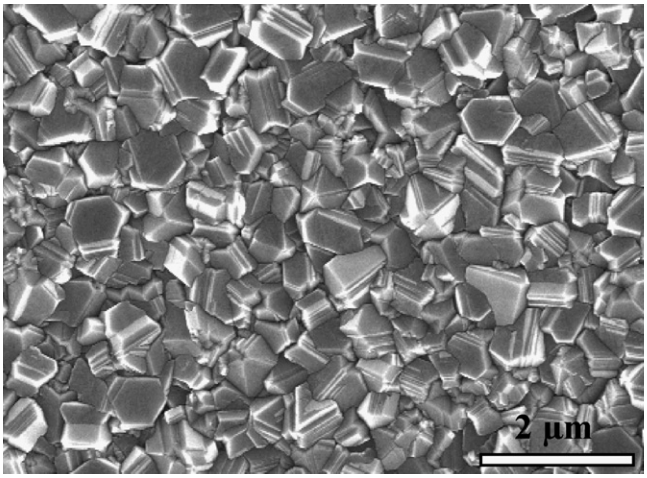

Fig. 7. SEM image of the diamond film deposited for 60 min.

3.5. Diamond growth with ND seeding

High-dense and homogenous ND layers seeded on the substrate will lead to high nucleation density, and faster coalescence between the crystallites. First, a short CVD growth (30 min, with parameters given in Section 2) was performed on ND seeding substrate.

The duration of the growth was limited to avoid an early coalescence of the crystals and clearly observe the growth of the nanoparticles. Fig. 6(a) shows the SEM images. A continuous diamond film was observed at the early stage of diamond growth. It can be seen that there are no visible pinholes in the film even at such a small grain size. The grain size is uniform across the film due to the even distribution of diamond nanoparticle.

In Fig. 6(b) of an enlargement SEM image, a growth of the nanoparticles clearly occurs. The particle size of nanodiamond seeds grew up to 200 nm, associated with faceting of the crystallites. The development of faceted diamond nanocrystal indicates

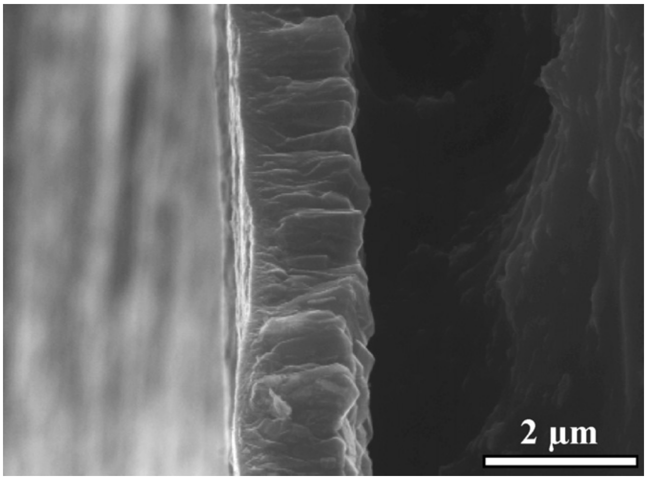

Fig. 8. Cross sectional image of the diamond film deposited for 60 min.

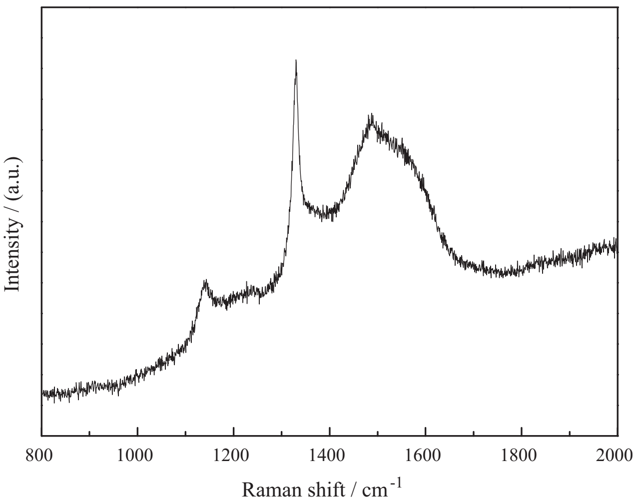

Fig. 9. Raman spectrum of the diamond film after diamond growth of 60 min.

diamond growth on the sp^3 seeds, which is commonly observed at the early stages of the CVD process [3].

When long CVD growth was performed (60 min), diamond film with well-faceted grains can be obtained, as shown in Fig. 7. Average crystal size was increased to 1 μm. From cross sectional image of the diamond film, a thickness about 750 nm was measured (Fig. 8). The growth rate is in agreement with the results obtained by other investigations, where bias-enhanced nucleation (BEN) process was adapted to enhance diamond nucleation [39].

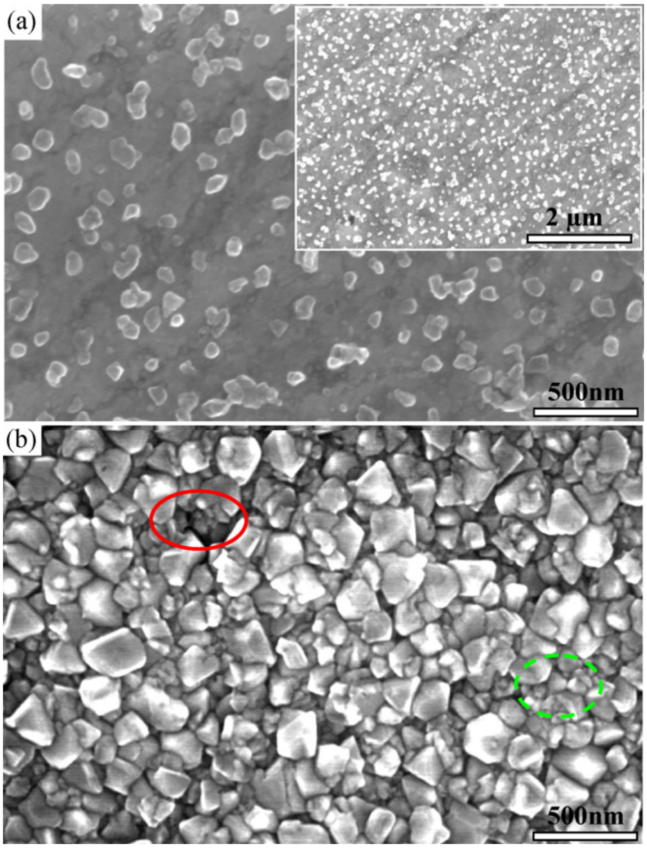

Fig. 10. (a) SEM image of two-dimensional self-assemblies of mono-crystalline seeding on Cu substrate, the inset is the SEM image at low-magnification; (b) SEM image of the diamond film deposited for 30 min.

The corresponding Raman spectrum is shown in Fig. 9. A major peak at 1330.17 cm^{-1} is corresponding to the diamond phase. The two other less resolved peaks at around 1138.26 and 1487.43 cm^{-1} are assigned to trans-polyacetylene segments at grain boundaries and surfaces, a characteristic of nanocrystalline diamond films [40].

The particle density by electrostatic self-assembly seeding certainly has great effect on CVD diamond growth. Due to small size of ND particle and rough surface of Cu substrate, there is comparatively large statistical error for particle number. We changed ND with bigger mono-crystalline diamond (average particle size is about 86.5 nm) and modified it with the same process described in Section 2. As shown in Fig. 10(a), the absorbed particle density is adjusted at about 2.9×10^9 cm^{-2} by electrostatic self-assembly seeding, which is a low limit for the nucleation of diamond film [41]. Subsequent diamond CVD growth is presented in Fig. 10(b). From the SEM image, we can investigate the effect of critical particle density on CVD diamond growth kinetics. This diamond film presents a transition state developing into a continuous film. There are two typical kinds of defects. One is caves (indicated with solid circle). The other is that heterogeneous nucleation seriously destroy the uniformity of crystal grains (indicated with dash circle). The reason is that diamond nucleated from pre-existing sp^3 seeds distributed on copper substrate has high growth rate than it nucleated from carbon aggregations.

4. Conclusion

After heat-treatment in air ambient, the oxidation of hydrocarbon groups on ND surface causes ND surface to be more negatively charged in de-ionized water. And as a result of increased electrostatic repulsion between these modified particles, the suspension becomes more stable and creates a larger portion of small particles. During electrostatic self-assembly seeding process, the attractive interaction energy between copper substrate and ND particles drove highly dispersed diamond seeds loaded tightly on substrate surface. Further CVD deposition showed that diamond nucleated from the two-dimensional self-assemblies of nanodiamond particles with short incubation time less than 30 min. High quality of 750 nm thick continuous diamond film was finally obtained in the growth time of 60 min. The particle density by electrostatic self-assembly seeding certainly has great effect on CVD diamond growth. Low density will cause two kinds of growth defects and decrease the quality of diamond film.

Appendix A.

The potential distribution in the diffusion-charged region between two interacting particles is governed by the well-known Poisson–Boltzmann equation, which is given by

$$\nabla^2\phi = \kappa^2 \sinh\phi \tag{1}$$

where the reduced potential ϕ is defined by

$$\phi = \frac{e\psi}{kT} \tag{2}$$

The Debye–Huckel constant κ is defined by

$$\kappa^2 = \frac{2e^2\sum_i z_i^2 N_i}{\varepsilon kT} \tag{3}$$

where N_i is the number per unit volume of ith electrolyte; z_i is the valences of the ion; e, ε, k and T have their usual meanings.

When the potential throughout the double layer is large compared to kT/e, about 25 mV at room temperature, the Poisson–Boltzmann equation cannot be linearized [42]. Then, we determined electrical double layer interaction energy of ND particle and copper substrate from the calculation of the electric double-layer force between unlike spheres described in [24].

If the dimensions of the plate surfaces are large enough, compared to the Debye–Huckel distance κ^{-1}, then ϕ depends only on coordinate x, where the axis is taken perpendicular to the interfacial planes. The Poisson–Boltzmann equation then becomes

$$\frac{d^2\phi}{dx^2} = \kappa^2 \sinh\phi \tag{4}$$

This equation can be integrated after multiplication by $d\phi/dx$, and the result may be expressed in the physically perspicuous form

$$2\eta kT(\cosh\phi - 1) - \frac{\varepsilon}{2}\left(\frac{kT}{e}\frac{d\phi}{dx}\right)^2 = \Im \tag{5}$$

Here, the constant $\Im$ thus represents the interaction force per unit area between the plates for the given potential distribution $\phi(x)$. Dividing Eq. (5) by $2\eta kT$, we can convert it to a dimensionless force density $\Im^+$.

$$\Im^+ = (\cosh\phi - 1) - \frac{\varepsilon}{4\eta kT}\left(\frac{kT}{e}\frac{d\phi}{dx}\right)^2 \tag{6}$$

If we define

$$g(\phi, \Im^+) = \sqrt{\left|2\cosh\phi - 2 - 2\Im^+\right|} \tag{7}$$

We can get the equation below

$$V^+(H) = -\Im^+\kappa H - \int_{\Phi_1}^{\Phi_2} g(\phi, \Im^+)d\phi + 4\left(cosh\frac{\Phi_1}{2} + \cosh\frac{\Phi_2}{2} - 2\right) \tag{8}$$

H is the separation distance of two particles. A dimensionless free energy of interaction can be defined by

$$V(H) = \frac{2\eta kTV^+(H)}{\kappa} \tag{9}$$

In Derjaguin's approximation, the spheres are divided into rings which are replaced by sections of plate perpendicular to the line of centers. It was shown by Hogg et al. that for unequal spheres this method gives the interaction force of electric double layer

$$f = \pi a' V(H) \tag{10}$$

where $\frac{1}{a'} = \frac{1}{2}\left(\frac{1}{a_1} + \frac{1}{a_2}\right)$, a_1 and a_2 are the radii of two unequal charged spheres. For the plate, $a_1 \to \infty$ then Eq. (10) becomes

$$f = 2\pi a_2 \frac{2\eta kT}{\kappa} V^+(H) \tag{11}$$

Finally, the interaction energy of electric double layer can be obtained by

$$V(H) = -\int_H^\infty f dH \tag{12}$$

References

[1] J.E. Butler, A.V. Sumant, The CVD of nanodiamond materials, Chem. Vap. Deposition 14 (2008) 145–160.
[2] A.A. Smolin, V.G. Ralchenko, S.M. Pimenov, T.V. Kononenko, E.N. Loubnin, Optical monitoring of nucleation and growth of diamond films, Appl. Phys. Lett. 62 (1993) 3449–3451.
[3] S. Iijima, Y. Aikawa, K. Baba, Early formation of chemical vapor deposition diamond films, Appl. Phys. Lett. 57 (1990) 2646–2648.
[4] O.A. Williams, O. Douhéret, M. Daenen, K. Haenen, E. Ōsawa, M. Takahashi, Enhanced diamond nucleation on monodispersed nanocrystalline diamond, Chem. Phys. Lett. 445 (2007) 255–258.
[5] H. Masuda, T. Yanagishita, K. Yasui, K. Nishio, I. Yagi, T.N. Rao, A. Fujishima, Synthesis of well-aligned diamond nanocylinders, Adv. Mater. 13 (2001) 247–249.
[6] S.-K. Lee, et al., Direct deposition of patterned nanocrystalline CVD diamond using an electrostatic self-assembly method with nanodiamond particles, Nanotechnology 21 (2010) 505302.
[7] H.A. Girard, S. Perruchas, C.l. Gesset, M. Chaigneau, L. Vieille, J.-C. Arnault, P. Bergonzo, J.-P. Boilot, T. Gacoin, Electrostatic grafting of diamond nanoparticles: a versatile route to nanocrystalline diamond thin films, ACS Appl. Mater. Interfaces 1 (2009) 2738–2746.
[8] I. Larionova, V. Kuznetsov, A. Frolov, O. Shenderova, S. Moseenkov, I. Mazov, Properties of individual fractions of detonation nanodiamond, Diamond Relat. Mater. 15 (2006) 1804–1808.
[9] E. Osawa, Recent progress and perspectives in single-digit nanodiamond, Diamond Relat. Mater. 16 (2007) 2018–2022.
[10] R.C. Mendes de Barros, E.J. Corat, N.G. Fereira, T.M. de Souza, V.J. Trava-Airoldi, N.F. Leite, K. Iha, Dispersion liquid properties for efficient seeding in CVD diamond nucleation enhancement, Diamond Relat. Mater. 5 (1996) 1323–1332.
[11] O. Shenderova, S. Hens, G. McGuire, Seeding slurries based on detonation nanodiamond in DMSO, Diamond Relat. Mater. 19 (2010) 260–267.
[12] L. Constant, F. Le Normand, HFCVD diamond nucleation and growth on polycrystalline copper: a kinetic study, Thin Solid Films 516 (2008) 691–695.
[13] L. Constant, C. Speisser, F. Le Normand, HFCVD diamond growth on Cu(111). Evidence for carbon phase transformations by in situ AES and XPS, Surf. Sci. 387 (1997) 28–43.
[14] C. Li, K.C. Feng, Y.J. Fei, H.T. Yuan, Y. Xiong, K. Feng, The influence of C-60 as intermediate on the diamond nucleation on copper substrate in HFCVD, Appl. Surf. Sci. 207 (2003) 169–175.
[15] N. Ali, W. Ahmed, C.A. Rego, Q.H. Fan, Combined substrate polishing and biasing during hot-filament chemical vapor deposition of diamond on copper, J. Mater. Res. 15 (2000) 593–595.
[16] E.D. Eidelman, V.I. Siklitsky, L.V. Sharonova, M.A. Yagovkina, A.Y. Vul, M. Takahashi, M. Inakuma, M. Ozawa, E. Ōsawa, A stable suspension of single ultrananocrystalline diamond particles, Diamond Relat. Mater. 14 (2005) 1765–1769.
[17] A. Krueger, M. Ozawa, G. Jarre, Y. Liang, J. Stegk, L. Lu, Deagglomeration and functionalisation of detonation diamond, Phys. Status Solidi (a) 204 (2007) 2881–2887.
[18] V. Nerapusri, J.L. Keddie, B. Vincent, I.A. Bushnak, Swelling, Deswelling of adsorbed microgel monolayers triggered by changes in temperature, pH, and electrolyte concentration, Langmuir 22 (2006) 5036–5041.
[19] Q.P. Wei, Z.M. Yu, L. Ma, D.F. Yin, J. Ye, The effects of temperature on nanocrystalline diamond films deposited on WC-13 wt.% Co substrate with W-C gradient layer, Appl. Surf. Sci. 256 (2009) 1322–1328.
[20] X.Y. Xu, Z.M. Yu, Y.W. Zhu, B.C. Wang, Influence of surface modification adopting thermal treatments on dispersion of detonation nanodiamond, J. Solid State Chem. 178 (2005) 688–693.
[21] O. Shenderova, I. Petrov, J. Walsh, V. Grichko, V. Grishko, T. Tyler, G. Cunningham, Modification of detonation nanodiamonds by heat treatment in air, Diamond Relat. Mater. 15 (2006) 1799–1803.
[22] X. Xu, Z. Yu, Y. Zhu, B. Wang, Effect of sodium oleate adsorption on the colloidal stability and zeta potential of detonation synthesized diamond particles in aqueous solutions, Diamond Relat. Mater. 14 (2005) 206–212.
[23] J.H. Kim, S.K. Lee, O.M. Kwon, S.I. Hong, D.S. Lim, Thickness controlled and smooth polycrystalline CVD diamond film deposition on SiO2 with electrostatic self assembly seeding process, Diamond Relat. Mater. 18 (2009) 1218–1222.
[24] G.M. Bell, G.C. Peterson, Calculation of the electric double-layer force between unlike spheres, J. Colloid Interface Sci. 41 (1972) 542–566.
[25] G.V. Lubarsky, S.A. Mitchell, M.R. Davidson, R.H. Bradley, van der, Waals interaction in systems involving oxidised polystyrene surfaces, Colloids Surf. A: Physicochem. Eng. Asp. 279 (2006) 188–195.
[26] M.N. Rahaman, Ceramic processing and sintering, Second Edition, CRC Press, New York, 2003.
[27] G. Michaèl, R. Stéphane, Robotic Micro-Assembly, John Wiley & Sons, New Jersey, 2010.
[28] W. Hongthani, N.A. Fox, D.J. Fermiĭn, Electrochemical properties of two dimensional assemblies of insulating diamond particles, Langmuir 27 (2011) 5112–5118.
[29] J.C. Arnault, S. Saada, M. Nesladek, O.A. Williams, K. Haenen, P. Bergonzo, E. Osawa, Diamond nanoseeding on silicon: stability under H2 MPCVD exposures and early stages of growth, Diamond Relat. Mater. 17 (2008) 1143–1149.
[30] G. Toikka, R.A. Hayes, Direct measurement of colloidal forces between mica and silica in aqueous electrolyte, J. Colloid Interface Sci. 191 (1997) 102–109.
[31] R.M. Pashley, DLVO and hydration forces between mica surfaces in Li+, Na+, K+, and Cs+ electrolyte solutions: a correlation of double-layer and hydration forces with surface cation exchange properties, J. Colloid Interface Sci. 83 (1981) 531–546.
[32] G. Toikka, R.A. Hayes, J. Ralston, Surface forces between zinc sulfide and silica in aqueous electrolyte, Colloids Surf. A: Physicochem. Eng. Asp. 141 (1998) 3–8.
[33] R.F. Considine, C.J. Drummond, Surface Roughness, Surface force measurement: a comparison of electrostatic potentials derived from atomic force microscopy and electrophoretic mobility measurements, Langmuir 17 (2001) 7777–7783.
[34] M. Giesbers, J.M. Kleijn, M.A. Cohen Stuart, The electrical double layer on gold probed by electrokinetic and surface force measurements, J. Colloid Interface Sci. 248 (2002) 88–95.
[35] J.-Y. Raty, G. Galli, C. Bostedt, T.W. van Buuren, L.J. Terminello, Quantum confinement and fullerenelike surface reconstructions in nanodiamonds, Phys. Rev. Lett. 90 (2003) 037401.
[36] G. Frens, Particle size and sol stability in metal colloids, Colloid Polym. Sci. 250 (1972) 736–741.

[37] O. Malysheva, T. Tang, P. Schiavone, Adhesion between a charged particle in an electrolyte solution and a charged substrate: electrostatic and van der Waals interactions, J. Colloid Interface Sci. 327 (2008) 251–260.

[38] D.Y.C. Chan, T.W. Healy, T. Supasiti, S. Usui, Electrical double layer interactions between dissimilar oxide surfaces with charge regulation and Stern–Grahame layers, J. Colloid Interface Sci. 296 (2006) 150–158.

[39] N. Ali, W. Ahmed, C.A. Rego, Q.H. Fan, Chromium interlayers as a tool for enhancing diamond adhesion on copper, Diamond Relat. Mater. 9 (2000) 1464–1470.

[40] A.C. Ferrari, J. Robertson, Origin of the 1150-cm-1 Raman mode in nanocrystalline diamond, Phys. Rev. B 63 (2001) 121405.

[41] J.G. Buijnsters, L. Vazquez, G.W.G. van Dreumel, J.J. ter Meulen, W.J.P. van Enckevort, J.P. Celis, Enhancement of the nucleation of smooth and dense nanocrystalline diamond films by using molybdenum seed layers, J. Appl. Phys. 108 (2010) 103514–103519.

[42] J. Stankovich, S.L. Carnie, Electrical double layer interaction between dissimilar spherical colloidal particles and between a sphere and a plate: nonlinear Poisson–Boltzmann theory, Langmuir 12 (1996) 1453–1461.